The Journal of Immunology

Lack of the Lectin-like Domain of Thrombomodulin Worsens Shiga Toxin-Associated Hemolytic Uremic Syndrome in Mice

Carlamaria Zoja, Monica Locatelli, Chiara Pagani, Daniela Corna, Cristina Zanchi, Berend Isermann, Giuseppe Remuzzi, Edward M. Conway and Marina Noris

J Immunol 2012; 189:3661-3668; Prepublished online 31 August 2012;
doi: 10.4049/jimmunol.1102118
http://www.jimmunol.org/content/189/7/3661

The Journal of Immunology is published twice each month by
The American Association of Immunologists, Inc.,
1451 Rockville Pike, Suite 650, Rockville, MD 20852

Print ISSN: 0022-1767 Online ISSN: 1550-6606.

Lack of the Lectin-like Domain of Thrombomodulin Worsens Shiga Toxin-Associated Hemolytic Uremic Syndrome in Mice

Carlamaria Zoja,*,[1] Monica Locatelli,*,[1] Chiara Pagani,* Daniela Corna,* Cristina Zanchi,* Berend Isermann,† Giuseppe Remuzzi,*,‡ Edward M. Conway,§ and Marina Noris¶

Shiga toxin (Stx)-producing *Escherichia coli* is a primary cause of diarrhea-associated hemolytic uremic syndrome (HUS), a disorder of thrombocytopenia, microangiopathic hemolytic anemia, and acute renal failure. The pathophysiology of renal microvascular thrombosis in Stx-HUS is still ill-defined. Based on evidence that abnormalities in thrombomodulin (TM), an anticoagulant endothelial glycoprotein that modulates complement and inflammation, predispose to atypical HUS, we assessed whether impaired TM function may adversely affect evolution of Stx-HUS. Disease was induced by coinjection of Stx2/LPS in wild-type mice ($TM^{wt/wt}$) and mice that lack the lectin-like domain of TM ($TM^{LeD/LeD}$), which is critical for its anti-inflammatory and cytoprotective properties. After Stx2/LPS, $TM^{LeD/LeD}$ mice exhibited more severe thrombocytopenia and renal dysfunction than $TM^{wt/wt}$ mice. Lack of lectin-like domain of TM resulted in a stronger inflammatory reaction after Stx2/LPS with more neutrophils and monocytes/macrophages infiltrating the kidney, associated with PECAM-1 and chemokine upregulation. After Stx2/LPS, intraglomerular fibrin(ogen) deposits were detected earlier in $TM^{LeD/LeD}$ than in $TM^{wt/wt}$ mice. More abundant fibrin(ogen) deposits were also found in brain and lungs. Under basal conditions, $TM^{LeD/LeD}$ mice exhibited excess glomerular C3 deposits, indicating impaired complement regulation in the kidney that could lead to local accumulation of proinflammatory products. $TM^{LeD/LeD}$ mice with HUS had a higher mortality rate than $TM^{wt/wt}$ mice. If applicable to humans, these findings raise the possibility that genetic or acquired TM defects might have an impact on the severity of microangiopathic lesions after exposure to Stx-producing *E. coli* infections and raise the potential for using soluble TM in the treatment of Stx-HUS. *The Journal of Immunology*, 2012, 189: 3661–3668.

The hemolytic uremic syndrome (HUS) consists of the triad of microangiopathic hemolytic anemia, thrombocytopenia, and acute renal failure. More than 85% of cases of HUS are preceded by a diarrheal illness triggered by strains of Shiga toxin (Stx)-producing *Escherichia coli* (STEC), mainly of serotype O157:H7 (1, 2). Enterohemorrhagic *E. coli* O157:H7, an emerging foodborne and water pathogen, has been the cause of multiple outbreaks, becoming a public health problem in both developed and developing countries (3–5). HUS with prodromal diarrhea occurs primarily in children and is a rare event in adults (6). However, a large outbreak (>4000 cases) of gastroenteritis and HUS belonging to an unusual (O104:H4), non-O157 STEC strain, predominantly affecting adults (89%), recently occurred in Germany (7). More than 25% of cases developed HUS, a proportion that is much higher than in previous outbreaks (8–10). The *E. coli* O104:H4 strain combines virulence potentials of enteroaggregative *E. coli* with a characteristic "stacked-brick" pattern of adherence to intestinal epithelial cells and of typical Stx-producing enterohemorrhagic *E. coli* (11). This unique and highly virulent enteric pathogen also acquired an extended-spectrum β-lactamase phenotype (7). This outbreak demonstrates that blended virulence profiles in enteric pathogens introduced into susceptible populations can have extreme clinical consequences (11) and highlights the need for effective treatments.

Indeed, apart from supportive therapy, there are currently no specific treatments for Stx-associated HUS (12). Strategies currently under investigation include STEC-component vaccines, Stx receptor mimics, and Abs against Stx (13). Encouraging data are emerging from the use of eculizumab, an mAb directed against the complement protein C5, as recently described in three children with severe Stx-associated HUS (14).

After STEC ingestion by contaminated food or water, Stx 1 and 2 are transported in the circulation to the capillary bed of target organs, such as the kidney and brain, that express the Gb3 receptor, thereby activating a cascade of signaling events leading to vascular dysfunction, leukocyte recruitment, and thrombus formation (reviewed in Ref. 15).

*Istituto di Ricerche Farmacologiche Mario Negri, Centro Anna Maria Astori, Parco Scientifico Tecnologico Kilometro Rosso, 24126 Bergamo, Italy; †Department of Clinical Chemistry and Pathobiochemistry, Otto-von-Guericke-University Magdeburg, 39120 Magdeburg, Germany; ‡Unità di Nefrologia e Dialisi, Azienda Ospedaliera Ospedali Riuniti di Bergamo, 24128 Bergamo, Italy; §Department of Medicine, Centre for Blood Research, University of British Columbia, Vancouver, British Columbia V6T 1Z3, Canada; and ¶Centro Ricerche Trapianti, "Chiara Cucchi De Alessandri e Gilberto Crespi", Istituto di Ricerche Farmacologiche Mario Negri, 24020 Ranica, Bergamo, Italy

[1]C.Z. and M.L. contributed equally to this work.

Received for publication July 20, 2011. Accepted for publication July 27, 2012.

This work was supported by a grant from Vereniging zonder winstoogmerk Zydeco, Waasmunster, Belgium, and a fellowship from "Fondazione Aiuti per la Ricerca sulle Malattie Rare", Bergamo, Italy (to M.L.). E.M.C. is an Adjunct Scientist with the Canadian Blood Services, holds a Canada Research Chair and a Commonwealth Serum Laboratories-Behring Research Chair in Endothelial Cell Biology, and is supported by the Canadian Institutes for Health Research (Grant 200978).

Address correspondence and reprint requests to Dr. Carlamaria Zoja, Mario Negri Institute for Pharmacological Research, Centro Anna Maria Astori, Science and Technology Park Kilometro Rosso, Via Stezzano, 87, 24126 Bergamo, Italy. E-mail address: carlamaria.zoja@marionegri.it

The online version of this article contains supplemental material.

Abbreviations used in this article: BUN, blood urea nitrogen; D+HUS, diarrhea-associated hemolytic uremic syndrome; HPF, high-power fields; HUS, hemolytic uremic syndrome; PMN, polymorphonuclear cell; STEC, Shiga toxin-producing *Escherichia coli*; Stx, Shiga toxin; TM, thrombomodulin; $TM^{LeD/LeD}$, mice that lack the lectin-like domain of TM; $TM^{wt/wt}$, wild-type mice.

Thrombomodulin (TM) is a transmembrane, endothelial glycoprotein receptor for thrombin, best known for its function as a cofactor in the protein C anticoagulant pathway (16). Beyond its role in coagulation, TM has properties that impact on fibrinolysis, complement activation, inflammation, and cell proliferation (17–19). Full-length TM comprises five structural domains, including a C-type lectin-like NH2-terminal module (Supplemental Fig. 1). Using transgenic mice that lack the lectin-like domain of TM ($TM^{LeD/LeD}$), it was shown that TM through its lectin-like domain interferes with inflammation by suppressing neutrophil adhesion to endothelial cells and dampening complement activation (20, 21). Mutations that impair the function of TM have been identified in patients with atypical HUS, a form not linked to STEC infection (19). Three of the six identified missense mutations were in the lectin-like domain of TM. In the same study, cultured cells expressing TM variants, including those involving the lectin-like domain, had diminished capacity to modulate complement activation as compared with cells transfected with wild-type TM, implying that TM mutations associated with atypical HUS cause defective complement regulation. There is in vitro evidence that TM expression was decreased in human glomerular microvascular endothelial cells exposed to Stx2 after presensitization with inflammatory mediators (22). More recently, in a mouse model of HUS induced by coinjection of Stx2 and LPS, reduced glomerular TM expression was observed in association with fibrin(ogen) and platelet deposition (23).

The earlier findings prompted us to investigate whether impaired TM function may adversely affect the evolution of Stx-associated HUS. To this end, we compared the course and severity of the disease in $TM^{LeD/LeD}$ mice as compared with wild-type mice ($TM^{wt/wt}$) in response to systemic administration of Stx2/LPS.

Materials and Methods

Experimental design

Male Swiss/129/sv/ev mice ($TM^{LeD/LeD}$) and age-matched Swiss/129/sv/ev $TM^{wt/wt}$ mice were generated by homologous recombination in embryonic stem cells as previously described (20) and bred in the animal facility of the Vesalius Research Center, University of Leuven, Leuven, Belgium, in accordance with the local institutional animal ethics committee. Mice were then maintained at Mario Negri Institute in conformity with the institutional guidelines that are in compliance with national and international laws and policies (23). All animal studies were approved by the Institutional Animal Care and Use Committees of Mario Negri Institute, Milan, Italy. HUS was induced in $TM^{wt/wt}$ and $TM^{LeD/LeD}$ mice (28–32 g body wt) by i.p. injection of Stx2 (200 ng/mouse; Toxin Technology, Sarasota, FL) plus LPS (75 μg/mouse, O111:B4; Sigma, St. Louis, MO) (23, 24). Mice were sacrificed at 3, 6, 24, or 48 h after Stx2/LPS injection. Groups of $TM^{wt/wt}$ and $TM^{LeD/LeD}$ mice were injected with saline and served as controls. For survival studies, $TM^{wt/wt}$ (n = 14) and $TM^{LeD/LeD}$ (n = 17) mice treated with Stx2/LPS were used. In additional experiments, $TM^{wt/wt}$ (n = 16) and $TM^{LeD/LeD}$ (n = 24) mice were treated with saline or low doses of Stx2 (10, 20 ng/mouse) plus LPS (75 μg/mouse), and sacrificed 24 or 48 h later. Blood platelet count and renal function measured by serum blood urea nitrogen (BUN, Reflotron test; Roche Diagnostic Corporation, Indianapolis, IN) were assessed. Kidneys were removed for immunohistochemical analysis and/or real-time PCR experiments, and brain and lungs for the evaluation of fibrin(ogen) deposits.

Immunohistochemical analysis

Kidney, brain, and lung tissues were immersed overnight in periodate lysine paraformaldehyde fixative at 4°C and then were transferred to 30% sucrose and frozen in OCT compound. Fibrin(ogen) staining was revealed by FITC-conjugated goat anti-rat fibrin(ogen) Ab (1:40; Nordic Immunology) using an inverted confocal laser microscope (LSM 510 meta; Zeiss, Jena, Germany). Nuclei and cell membranes were stained with DAPI (blue) and rhodamine wheat germ agglutinin-lectin (red; Vector Laboratories), respectively. Negative controls were obtained using FITC-conjugated polyclonal goat Ab (1:40; Nordic Immunology) on adjacent sections. Fibrin(ogen) expression was estimated using ImageJ software. C3 deposits were evaluated in acetone-fixed frozen sections (3 μm) by staining with FITC-conjugated goat anti-mouse C3 Ab (10 μg/ml; Cappel). Glomerular C3 staining was scored from 0 to 3: 0, no staining or traces (<5%); 1, staining in <25% of the glomerular tuft; 2, staining affecting 26–50%; 3, staining >50%. Polymorphonuclear cells (PMNs) were revealed in renal OCT-frozen sections by monoclonal rat anti-mouse Ly-6B.2 alloantigen Ab (1:400; AbD Serotec). PMNs were counted for each glomerulus and in randomly selected high-power fields (HPF) of interstitial areas (×400). Ab against a cytoplasmic Ag present in mouse monocytes/macrophages (F4/80, 2.5 μg/ml; Caltag Laboratories) was used for the detection of mononuclear cells by immunoperoxidase technique in Duboscq-Brazil–fixed and paraffin-embedded sections. $F4/80^+$ cells were counted in randomly selected HPF (×400) of interstitial areas. PECAM-1 was detected in OCT-frozen sections using rat anti-mouse Ab (1:50, BD Biosciences) followed by FITC-conjugated goat anti-rat IgG (1:150; Sigma). Negative controls were obtained using rat IgG2a isotype control (1:1600; BD Biosciences) on adjacent sections. Glomerular and peritubular expression was estimated by ImageJ software. MIP-2/CXCL2 expression was evaluated in acetone-fixed frozen sections by staining with goat anti-mouse MIP-2 Ab (1:250; Santa Cruz). MIP-2 expression was estimated by ImageJ software. MCP-1/CCL2 expression was detected by goat polyclonal anti–MCP-1 Ab (1:100; Santa Cruz) using avidin/biotin complex immunoperoxidase on paraffin-embedded tissue. Negative controls were obtained by omitting the primary Ab on adjacent sections. MCP-1 immunostaining in the cortical tubulointerstitium was expressed as number of positive tubuli/HPF (×400).

Quantitative real-time PCR

Total RNA was isolated from kidney tissue using TRIzol reagent (Invitrogen). Purified RNA (2 μg) was reverse transcribed. Amplification was performed on 7300 Real-Time PCR System (Life Technologies) using TaqMan Universal PCR Master Mix and inventoried TaqMan assay Mn00436450_m1 for mouse MIP2/CXCL2, Mn99999056_m1 for mouse MCP-1, and a mouse β-actin endogenous control (VIC/MGB probe) as reference gene. The ΔΔCt method was used to calculate relative changes in expression of target genes in respect to a calibrator sample (untreated $TM^{wt/wt}$).

Statistical analysis

Results are expressed as mean ± SE. Data were analyzed by the nonparametric Mann–Whitney or Kruskal–Wallis tests or by ANOVA where appropriate. Survival curves were analyzed by the log-rank test. Statistical significance level was defined as $p < 0.05$.

Results

Thrombocytopenia and renal function impairment after Stx2/LPS are more severe in $TM^{LeD/LeD}$ mice

Under baseline conditions, $TM^{wt/wt}$ and $TM^{LeD/LeD}$ mice had normal platelet counts and renal function (Fig 1A, 1B). A decrease in the platelet count was observed in $TM^{wt/wt}$ mice treated with Stx2 (200 ng/mouse) plus LPS (75 μg/mouse) (23) at 24 and 48 h compared with baseline (45 and 63% reduction, respectively; Fig. 1A). However, the thrombocytopenia was accentuated in mice that lack the lectin-like domain (54 and 77% reduction at 24 and 48 h versus basal), with a significant ($p < 0.05$) difference in platelet count between $TM^{LeD/LeD}$ and $TM^{wt/wt}$ mice. Renal function was impaired in $TM^{wt/wt}$ mice treated with Stx2/LPS, as indicated by increased serum BUN levels (Fig. 1B). After exposure to Stx2/LPS, renal function was worse in $TM^{LeD/LeD}$ mice, represented by significantly higher BUN levels as compared with $TM^{wt/wt}$ mice (24 h, $p < 0.01$; 48 h, $p < 0.05$; Fig. 1B).

The highest susceptibility of $TM^{LeD/LeD}$ mice to develop renal function impairment was observed also when consistently lower doses of Stx2 were given (Table I). Thus, whereas in $TM^{wt/wt}$ mice only a mild increase in BUN levels was observed after 20 ng Stx2, $TM^{LeD/LeD}$ mice showed a significant increase in serum BUN levels at 24 ($p < 0.01$) and 48 h ($p < 0.05$) with respect to baseline. Notably, in $TM^{LeD/LeD}$ mice, BUN levels were significantly higher than those measured in the $TM^{wt/wt}$ mice (24 h, $p <$ 0.05). A trend toward increase was observed in $TM^{LeD/LeD}$ mice after 10 ng Stx2, which, however, did not reach statistical sig-

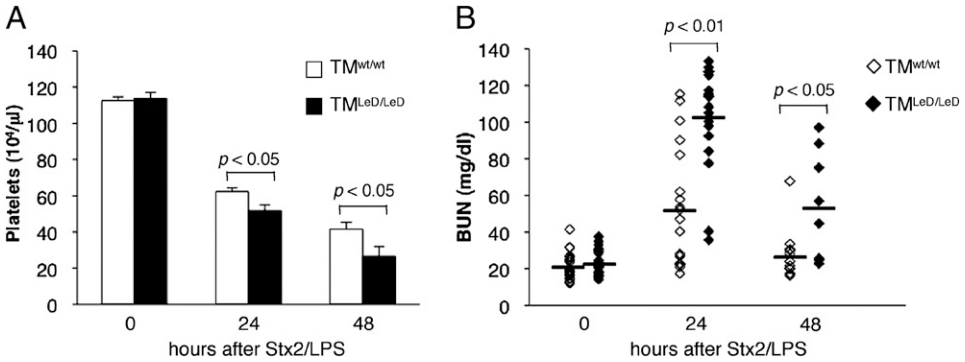

FIGURE 1. Platelet count and renal function in $TM^{wt/wt}$ and $TM^{LeD/LeD}$ mice treated with Stx2 plus LPS. (**A**) $TM^{LeD/LeD}$ mice exhibited more severe thrombocytopenia compared with $TM^{wt/wt}$ mice. (**B**) Lack of the lectin-like TM domain worsened the decline of renal function, assessed as BUN levels. Data are mean ± SE (n = 25 mice/group at time 0; n = 20 mice/group at 24 h; n = 11 mice/group at 48 h).

nificance (Table I). Platelet count was reduced by 42 ± 4.4% in $TM^{LeD/LeD}$ mice after 20 ng Stx2/LPS as compared with 22 ± 2.5% reduction in $TM^{wt/wt}$ mice at 24 h ($p < 0.05$).

Glomerular and interstitial inflammatory reaction in $TM^{LeD/LeD}$ mice after Stx2/LPS

We quantified PMN and monocyte/macrophage infiltration into the kidneys of $TM^{wt/wt}$ and $TM^{LeD/LeD}$ mice before and after Stx2/LPS treatment. Before Stx2, there was no genotype-dependent difference in the number of glomerular or interstitial PMNs, as quantified after immunofluorescence staining of histologic sections (Fig. 2A, 2B). However, after Stx2/LPS, the number of PMNs in the glomeruli and interstitium of $TM^{LeD/LeD}$ mice was significantly increased as compared with $TM^{wt/wt}$ mice (Fig. 2A, 2B). Accumulation of $F4/80^+$ monocytes/macrophages in the renal interstitium was 2-fold higher under basal conditions in $TM^{LeD/LeD}$ mice as compared with $TM^{wt/wt}$ mice ($p < 0.05$). Similar to the findings with PMNs, Stx2/LPS injection induced greater accumulation of monocytes/macrophages in the renal interstitium of $TM^{LeD/LeD}$ versus $TM^{wt/wt}$ mice (24 h, $p < 0.05$; Fig. 2C).

We evaluated the expression of PECAM-1, a multifunctional adhesion and signaling molecule involved in transendothelial migration of neutrophils and monocytes (25–27). PECAM-1 was constitutively expressed by glomerular endothelial cells and peritubular capillaries in the kidneys of both $TM^{wt/wt}$ and $TM^{LeD/LeD}$ mice, although the staining was more intense and diffuse in $TM^{LeD/LeD}$ mice ($p < 0.05$; Fig. 3A). After Stx2/LPS treatment, the lack of the lectin-like domain of TM resulted in a further increase in expression of PECAM-1 compared with $TM^{wt/wt}$ mice ($p < 0.05$; Fig. 3A). No signal was observed when renal sections were stained with isotype primary Ab control (Supplemental Fig. 2A).

Next, we investigated the expression of chemokines allowing neutrophil and macrophage recruitment in the Stx2/LPS model, specifically, MIP-2/CXCL2 and MCP-1/CCL2 (28, 29). Chemokine mRNA was evaluated in renal tissue using quantitative real-time PCR. After Stx2/LPS injection, 176- and 264-fold increases in MIP2/CXCL2 mRNA were observed at 6 h in $TM^{wt/wt}$ and $TM^{LeD/LeD}$ mice, respectively, as compared with untreated mice (Fig. 4A). MCP-1 mRNA expression increased by 103-fold in the kidney of $TM^{wt/wt}$ mice treated with Stx2/LPS with respect to control mice. In $TM^{LeD/LeD}$ mice, MCP-1 levels were 230-fold higher than untreated mice ($p < 0.05$ versus $TM^{wt/wt}$; Fig. 4B). As shown in Fig. 3B, MIP-2 staining was minimal in the kidneys of untreated $TM^{wt/wt}$ and $TM^{LeD/LeD}$ mice. MIP-2 staining at periglomerular and tubular levels was observed within 6 h after Stx2/LPS administration in both groups of mice, with more intensity in $TM^{LeD/LeD}$ mice ($p < 0.05$). Constitutive expression of MCP-1 was detected in the proximal tubuli of $TM^{LeD/LeD}$ mice (Fig. 3C). After challenge with Stx2/LPS, MCP-1 staining was evident in $TM^{wt/wt}$ mice at 6 h, but it was more abundant in $TM^{LeD/LeD}$ mice ($p < 0.01$).

Lack of the lectin-like domain of TM favors glomerular prothrombotic state after Stx2/LPS

Under baseline conditions, kidneys from $TM^{wt/wt}$ and $TM^{LeD/LeD}$ mice exhibited minimal or undetectable amounts of fibrin(ogen) deposition in the glomerular capillaries (Fig. 5A). At 3 h after Stx2/LPS injection, there were only traces of fibrin(ogen) in $TM^{wt/wt}$ kidneys, whereas staining became more prominent starting at 6 h (Fig. 5A). In contrast, in $TM^{LeD/LeD}$ mice, the deposition of fibrin(ogen) in response to Stx2/LPS became readily evident at the early time point of 3 h and was more abundant than in $TM^{wt/wt}$ mice at 6 h. As shown by quantification analysis (Fig. 5A), a significant difference in fibrin(ogen) deposition between the two groups of mice persisted at 24 and 48 h. No signal was found when renal sections were stained with control Ab (Supplemental Fig. 2B).

Table I. Serum BUN levels in $TM^{wt/wt}$ mice and $TM^{LeD/LeD}$ mice treated with low doses of Stx2 plus LPS

Groups	Mean BUN ± SE (mg/dl)		
	Baseline	24 h	48 h
$TM^{wt/wt}$ mice			
Stx2 (20 ng)/LPS	19.05 ± 1.01 (n = 8)	28.54 ± 5.81 (n = 8)	30.53 ± 7.08 (n = 4)
Stx2 (10 ng)/LPS	19.62 ± 1.51 (n = 5)	24.70 ± 4.10 (n = 5)	29.15 ± 3.35 (n = 3)
$TM^{LeD/LeD}$ mice			
Stx2 (20 ng)/LPS	19.21 ± 1.03 (n = 10)	45.97 ± 8.20*, ** (n = 10)	38.52 ± 7.32*** (n = 5)
Stx2 (10 ng)/LPS	18.60 ± 2.57 (n = 10)	34.46 ± 13.41 (n = 10)	32.76 ± 11.49 (n = 5)

*$p < 0.01$ versus corresponding baseline; **$p < 0.05$ versus $TM^{wt/wt}$ at 24 h; ***$p < 0.05$ versus corresponding baseline.

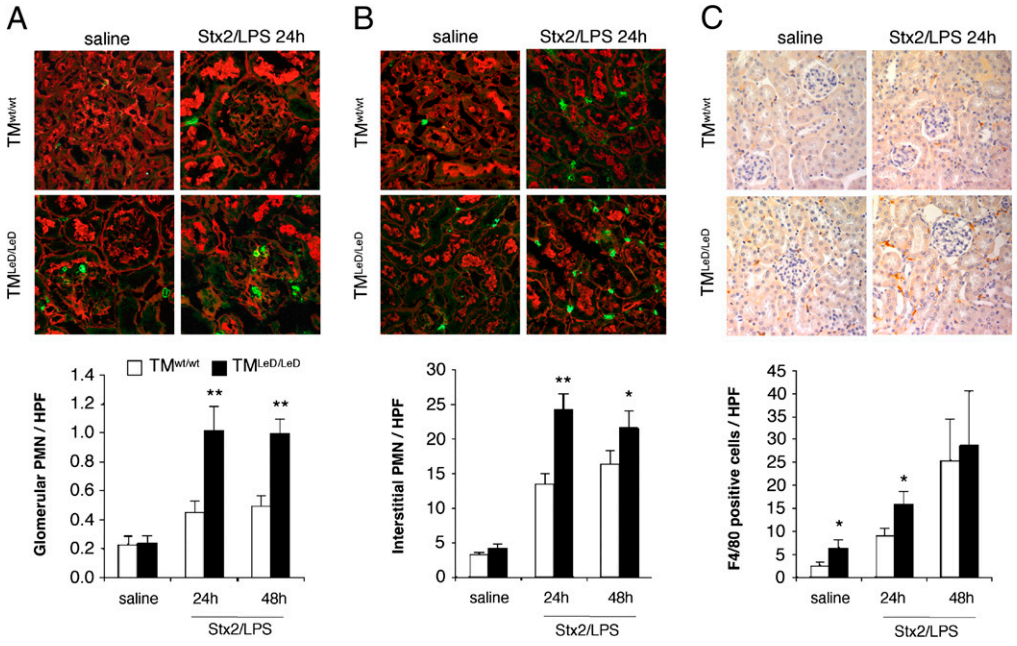

FIGURE 2. $TM^{LeD/LeD}$ mice had a stronger kidney inflammatory reaction after Stx2/LPS than $TM^{wt/wt}$ mice. (**A**) Accumulation of PMNs in the glomeruli (original magnification ×630) and (**B**) in the renal interstitium (original magnification ×400); (**C**) infiltrates of $F4/80^+$ monocytes/macrophages in the renal interstitium of $TM^{wt/wt}$ and $TM^{LeD/LeD}$ mice treated with saline or Stx2 plus LPS (original magnification ×400). PMNs were revealed by immunofluorescence, and counted for each glomerulus and in randomly selected HPF of interstitial areas (×400). $F4/80^+$ cells were counted in randomly selected HPF (×400) of interstitial areas. Data are mean ± SE of n = 7–9 mice/group. $*p < 0.05$, $**p < 0.01$ versus $TM^{wt/wt}$ mice.

Histologic sections of kidneys from untreated $TM^{wt/wt}$ mice that were immunostained for C3 revealed staining along Bowman's capsule (23, 30) and minimal focal staining in the glomeruli (score: 0.45 ± 0.09; Fig. 5B). Under the same basal conditions, there was notably more C3 deposition within the glomeruli of $TM^{LeD/LeD}$ mice ($p < 0.01$). The findings are consistent with spontaneous complement activation in the $TM^{LeD/LeD}$ kidneys, which could favor the development of a glomerular prothrombotic state after HUS induction. At 24 h after Stx2/LPS injection, glomerular C3 staining was significantly ($p < 0.01$) increased in $TM^{wt/wt}$ mice, as compared with $TM^{wt/wt}$ mice treated with saline. $TM^{LeD/LeD}$ mice also responded to Stx2/LPS with an increase in glomerular C3 deposits ($p < 0.05$ versus saline), but the amount of C3 staining was not different from that observed in Stx2/LPS-treated $TM^{wt/wt}$ mice (Fig. 5B). When mice were exposed at a lower dose of Stx2 (20 ng) plus LPS, we could appreciate at 24 h a slight increase in C3 deposition only in $TM^{LeD/LeD}$ mice, which, however, did not reach a statistical significance as compared with glomerular C3 deposits under basal condition (Supplemental Fig. 3).

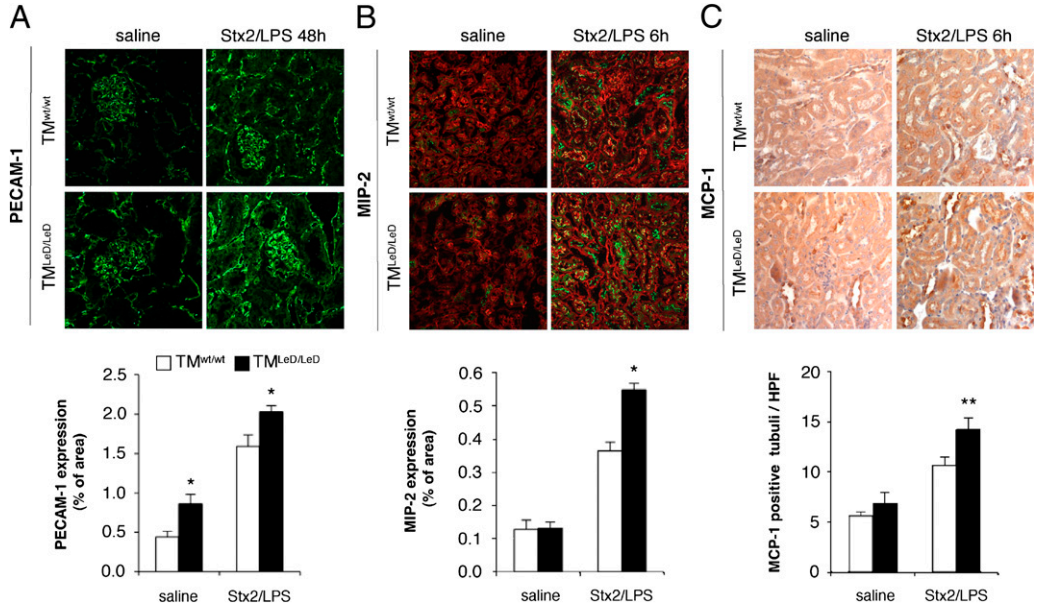

FIGURE 3. Renal expression of PECAM-1, MIP-2, and MCP-1 is higher in $TM^{LeD/LeD}$ mice than $TM^{wt/wt}$ mice in response to Stx2/LPS. Representative images and quantification of (**A**) PECAM-1, (**B**) MIP-2, and (**C**) MCP-1 staining in the kidney of $TM^{wt/wt}$ and $TM^{LeD/LeD}$ mice treated with saline or Stx2/LPS (n = 6 mice/group). Original magnification ×400. Data are mean ± SE. $*p < 0.05$, $**p < 0.01$ versus $TM^{wt/wt}$ mice.

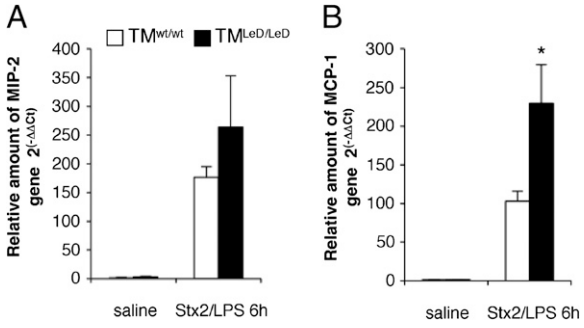

FIGURE 4. Chemokine mRNA expression in the kidneys of $TM^{wt/wt}$ and $TM^{LeD/LeD}$ mice 6 h after Stx2/LPS injection. Levels of (**A**) MIP2/CXCL2 and (**B**) MCP-1/CCL2 were determined by real-time PCR. Data are mean ± SE. $*p < 0.05$ versus $TM^{wt/wt}$ mice.

Fibrin(ogen) deposits in brain and lungs of $TM^{LeD/LeD}$ mice treated with Stx2/LPS

Extrarenal manifestations of diarrhea-associated HUS (D+HUS) are increasingly being recognized, with the most common organ affected being the brain (31–33). Indeed, neurologic involvement in HUS may be an important determinant of morbidity and mortality. Pulmonary involvement, although less common, has also been reported in HUS (34). In both of these organs, histopathologic studies from fatal cases of HUS have revealed the presence of microthrombi (32, 35). We therefore examined the brain and lungs of Stx2/LPS-treated $TM^{wt/wt}$ and $TM^{LeD/LeD}$ mice for fibrin (ogen) staining. Representative images and quantification data are shown in Fig. 6. Consistent with the notion that the lectin-like domain of TM reduces the sensitivity of mice to the thrombotic microangiopathy associated with D+HUS, there was more abundant fibrin(ogen) deposition in the brain (Fig. 6A) and lungs (Fig. 6B) of $TM^{LeD/LeD}$ mice compared with $TM^{wt/wt}$ mice, as evaluated 24 and 48 h after Stx2/LPS injection.

Lack of the lectin-like domain of TM increases mortality in a murine model of HUS

The induction of HUS by Stx2/LPS resulted in the death of >50% of $TM^{LeD/LeD}$ mice within 54 h, whereas only 20% of $TM^{wt/wt}$ mice died during the same period (Fig. 7A). At 120 h, when all the $TM^{LeD/LeD}$ mice had died, 29% of $TM^{wt/wt}$ mice were still alive (Fig. 7A). The difference in survival between the two groups was statistically significant ($p < 0.01$), confirming the enhanced sensitivity of the $TM^{LeD/LeD}$ mice to Stx2/LPS-HUS associated mortality. Moreover, although both $TM^{wt/wt}$ and $TM^{LeD/LeD}$ mice progressively lost weight after injection of the Stx2/LPS (Fig. 7B), the reduction was significantly greater in the $TM^{LeD/LeD}$ mice.

Discussion

This study demonstrates that lack of the lectin-like domain of TM in mice increases their sensitivity to manifesting the phenotypic changes in a model of Stx-HUS. Thus, after exposure to Stx2/LPS, $TM^{LeD/LeD}$ mice develop more severe thrombocytopenia and renal function impairment, earlier and more abundant glomerular fibrin (ogen) deposits, and increased mortality. The findings are consistent with the important role that TM plays as an anticoagulant and anti-inflammatory molecule in the microvasculature, particularly in the setting of Stx-mediated injury. We have already shown that TM mutations in humans increase the risk for development of

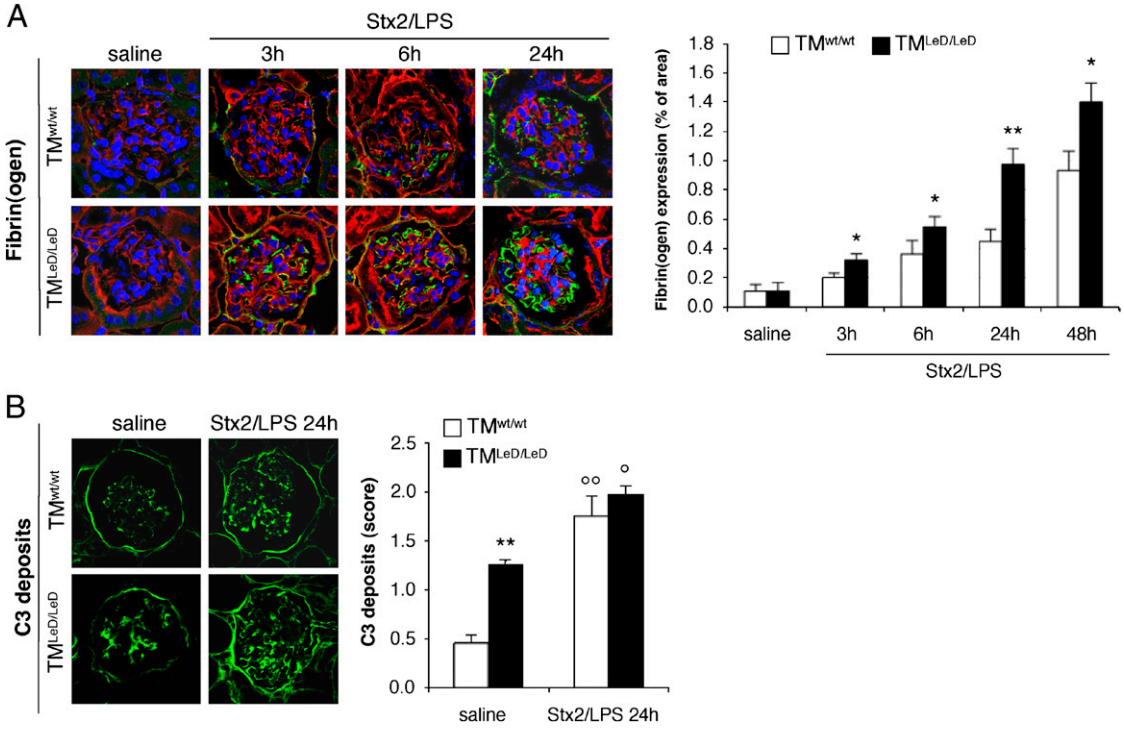

FIGURE 5. Fibrin(ogen) and C3 deposits in glomeruli of $TM^{wt/wt}$ and $TM^{LeD/LeD}$ mice treated with saline or Stx2 plus LPS. (**A**) Fibrin(ogen) deposits (green) were detected in the kidney of $TM^{LeD/LeD}$ mice earlier than in $TM^{wt/wt}$ mice in response to Stx2/LPS injection. Nuclei and cell membranes were detected with DAPI (blue) and rhodamine wheat germ agglutinin-lectin (red), respectively. Fibrin(ogen) staining was detected by confocal microscopy. Representative images and quantification of the fibrin(ogen) deposits at different time points are shown; $n = 6$ mice/group. Original magnification ×630. Data are mean ± SE. $*p < 0.05$, $**p < 0.01$ versus $TM^{wt/wt}$ mice. (**B**) Excessive C3 deposits were present in glomeruli of $TM^{LeD/LeD}$ mice on saline with respect to $TM^{wt/wt}$ mice. As shown in representative images and in the quantification graph, under basal conditions, there was more C3 deposition within the glomeruli of $TM^{LeD/LeD}$ mice. After Stx2/LPS injection, C3 staining was similar in the two groups ($n = 6$ mice/each group). Original magnification ×630. Data are mean ± SE. $**p < 0.01$ versus $TM^{wt/wt}$ mice; $^{\circ}p < 0.05$, $^{\circ\circ}p < 0.01$ versus corresponding saline.

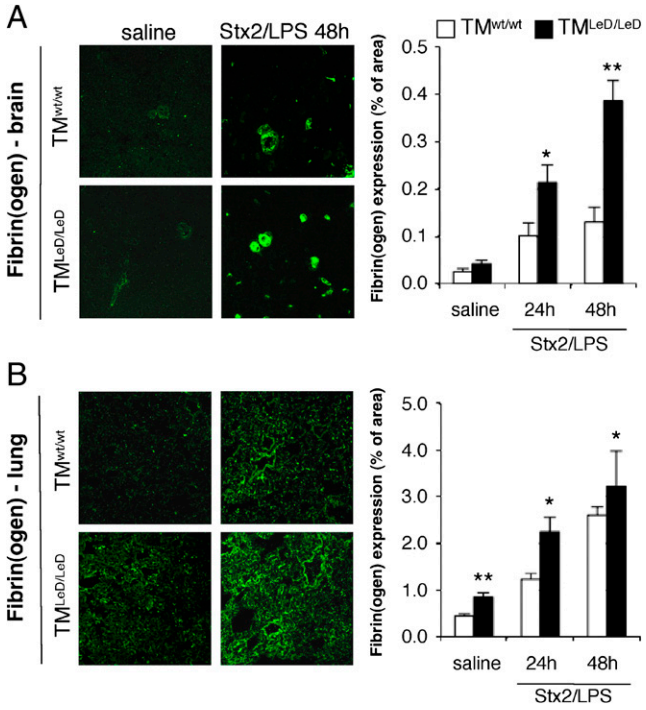

FIGURE 6. In brain and lung of $TM^{LeD/LeD}$ mice, more prominent fibrin (ogen) staining was detected after Stx2/LPS injection compared with $TM^{wt/wt}$ mice. Representative images and quantification of fibrin(ogen) staining in (**A**) brain and (**B**) lung of $TM^{wt/wt}$ and $TM^{LeD/LeD}$ mice treated with saline or Stx2/LPS (24, 48 h). Fibrin(ogen) staining was detected by confocal microscopy. Original magnification ×630 (A) and ×400 (B). Data are mean ± SE of $n = 6$ mice/each group. $*p < 0.05$, $**p < 0.01$ versus $TM^{wt/wt}$ mice.

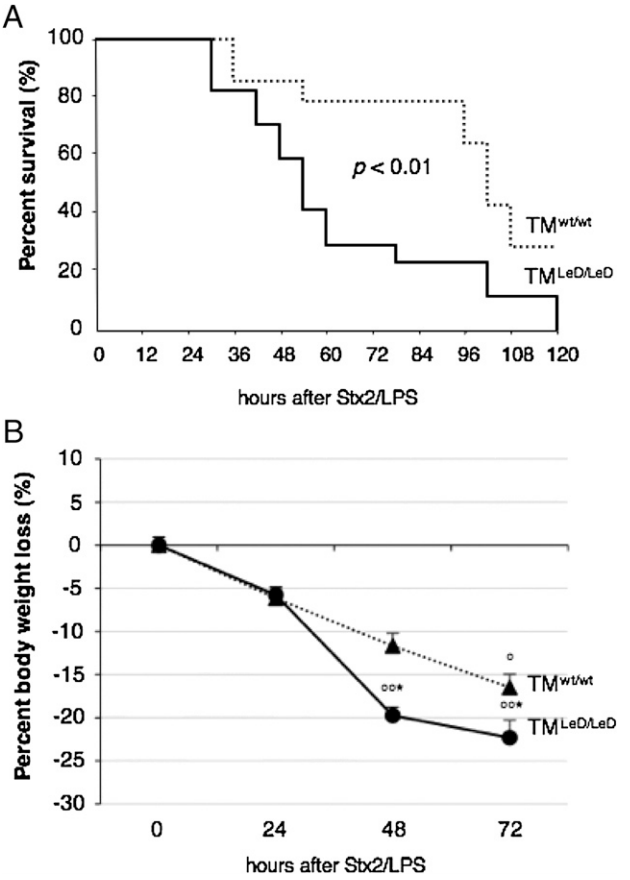

FIGURE 7. Influence of the lack of lectin-like domain of TM on survival and body weight of HUS mice. (**A**) Survival and (**B**) weight loss of $TM^{wt/wt}$ ($n = 14$) and $TM^{LeD/LeD}$ ($n = 17$) mice treated with Stx2/LPS. Lack of the lectin-like TM domain increased mortality of HUS mice. Data are mean ± SE. $*p < 0.01$ versus $TM^{wt/wt}$ (log-rank test). After Stx2 plus LPS injection, the percentage of total body weight loss was greater in $TM^{LeD/LeD}$ than $TM^{wt/wt}$ mice. Data are mean ± SE. $^{\circ}p < 0.05$, $^{\circ\circ}p < 0.01$ versus corresponding time 0; $*p < 0.05$ versus $TM^{wt/wt}$.

atypical HUS (19) (i.e., not Stx-associated). If our current findings are applicable to humans, it is reasonable to consider that genetic or acquired functional defects in TM may also contribute to an adverse outcome during the course of Stx-associated HUS.

TM is a 557-aa endothelial glycoprotein that is anchored to the cell by a short cytoplasmic tail and a single transmembrane domain (36). A stretch of six epidermal growth factor-like repeats support thrombin-mediated generation of activated protein C, which has anticoagulant and anti-inflammatory properties, and generation of activated thrombin activatable fibrinolysis inhibitor that also inactivates complement-derived anaphylatoxins C3a and C5a. Farthest from the membrane is the lectin-like domain of TM that has distinct anti-inflammatory properties, interfering with neutrophil and monocyte adhesion to endothelial cells, suppressing activation of MAPK and NF-κB pathways, interfering with complement activation (20, 21), and blocking the activity of the proinflammatory cytokine high mobility group box 1 (37). $TM^{LeD/LeD}$ mice accumulated more neutrophils in the lung, had higher serum cytokine levels, and had reduced survival (20) in response to endotoxemia. Similarly, after myocardial ischemia/reperfusion, $TM^{LeD/LeD}$ mice developed larger infarcts than $TM^{wt/wt}$, associated with more intense neutrophil extravasation within the ischemic regions (20). Finally, $TM^{LeD/LeD}$ mice had enhanced sensitivity to develop inflammatory arthritis that was associated with augmented monocyte/macrophage accumulation into joints (21). Administration of recombinant lectin-like domain of TM protected $TM^{LeD/LeD}$ mice against these insults (20, 38). Consistently, in this study, we found that after Stx2/LPS treatment, $TM^{LeD/LeD}$ mice exhibited a stronger inflammatory reaction in the kidney than the $TM^{wt/wt}$, with a higher number of neutrophils infiltrating the glomeruli and renal interstitium. Interstitial accumulation of monocytes/macrophages was also more abundant. There is considerable evidence that neutrophils and monocytes play an active role in the pathogenesis of Stx-associated HUS, and that their interactions with activated endothelial cells serve to amplify microvascular injury in the kidney (15). During the acute phase of D+HUS, neutrophils are activated, become more adhesive, and damage the endothelium by producing α1-antitrypsin–complexed elastase (39, 40). Kidney biopsies from D+HUS children showed mononuclear and PMNs within the glomeruli, along the zone of microvascular injury (41, 42). In vitro, Stx promoted leukocyte adhesion and transmigration across glomerular endothelial cells via upregulation of adhesion molecules and chemokines (24, 43). In $TM^{LeD/LeD}$ mice, the increased accumulation of leukocytes in the kidneys after Stx2/LPS injection was associated with overexpression of PECAM-1, a transmembrane glycoprotein belonging to the Ig superfamily of adhesion molecules with functional roles in leukocyte transendothelial cell migration (25, 26). PECAM-1 is expressed at high density at the lateral borders of endothelial cells and at a lower density on the surface of hematopoietic and immune cells, including neutrophils, monocytes, and platelets (27). Endothelial PECAM-1 facilitates leukocyte transmigration through homophilic interactions with leukocyte PECAM-1 and heterophilic interactions with neutrophil CD177 (25, 26). Studies with blocking Abs or inactivation of the PECAM-1 gene indicate that the role of this protein in modulating leukocyte infiltration in inflamed tissues strongly depends on the

stimulus and the experimental model used (26, 27). There is evidence showing that in a mouse model of HUS (28, 29), chemokines, including MIP-2 and MCP-1, are critical effectors of Stx-associated renal inflammation. In this study, we found that these chemokines were expressed at more extent in the kidneys of $TM^{LeD/LeD}$ than $TM^{wt/wt}$ mice after Stx2/LPS, indicating that they may contribute to the exuberant accumulation of PMNs and monocyte/macrophages in $TM^{LeD/LeD}$ mice.

We recently documented that complement activation via the alternative pathway plays a major role in mediating Stx-induced microvascular injury and thrombosis (23). By in vitro experiments, we found that Stx induced C3 activation and deposition on the surface of human microvascular endothelial cells, which was, in turn, instrumental in thrombus formation. Stx2/LPS treatment in mice was associated with intense C3 deposits in the glomeruli, and factor B-deficient mice that cannot activate the alternative pathway of complement were protected from thrombocytopenia and renal function impairment after Stx2/LPS (23). TM has been shown to negatively regulate C3 activation via the alternative pathway in vitro by accelerating factor I-mediated inactivation of C3b in the presence of the cofactor CFH (19). The TM variants found in patients with atypical HUS and affecting the lectin-like domain had diminished capacity to inactivate C3b (19), indicating that this domain is important for TM-complement regulatory properties. In line with these findings, we previously demonstrated that there is excessive C3 deposition in the articular joints of $TM^{LeD/LeD}$ mice under basal conditions as compared with $TM^{wt/wt}$ mice (21). Our data that $TM^{LeD/LeD}$ mice also have more glomerular C3 deposits under basal conditions would indicate impaired complement regulation in these mice and supports a role for the lectin-like domain of TM in preventing spontaneous complement activation in several organs, including the kidney. Enhanced baseline complement activation in $TM^{LeD/LeD}$ mice may contribute to the more rapid onset and increased severity of disease after Stx2/LPS, by facilitating accumulation of proinflammatory products, such as C3b and C5b-9, and of the anaphylatoxins C3a/C5a that mediate the recruitment of inflammatory cells. Of note, we found no difference in glomerular C3 deposits between $TM^{LeD/LeD}$ and $TM^{wt/wt}$ mice after Stx2/LPS injection, which is in line with our previous observation that at day 6 after collagen Ab-induced arthritis, when clinical signs were worse in the $TM^{LeD/LeD}$ mice, complement deposits were similarly increased in $TM^{LeD/LeD}$ and $TM^{wt/wt}$ mice (21). The earlier observations would suggest that maximal complement stimulation induced by Stx2/LPS (23) or by collagen Abs (44, 45) overwhelms the complement regulatory activity of the lectin-like domain of TM.

In conclusion, we have shown that after Stx2/LPS induction of HUS, $TM^{LeD/LeD}$ mice as compared with $TM^{wt/wt}$ mice exhibit more severe and earlier onset disease, with a shortened survival time. The accelerated renal microvascular injury in the $TM^{LeD/LeD}$ mice may reasonably be attributed to increased accumulation of inflammatory cells and overactivation of complement in the renal glomeruli. The Stx2/LPS-treated $TM^{LeD/LeD}$ mice also developed changes associated with thrombotic microangiopathic lesions in the brain and lung. These findings are consistent with those in humans with D+HUS and the fact that the Stx receptor Gb3 is expressed in the brain and lungs (46, 47), and help to explain the reduced survival of the $TM^{LeD/LeD}$ mice. Our findings are rationale for determining whether TM gene variants in humans are associated with increased risk for the development of HUS upon STEC infection. This report also raises the possibility that recombinant soluble TM might have therapeutic efficacy in HUS. Indeed, in a phase 3 clinical trial for disseminated intravascular coagulation (48), recombinant soluble TM has been shown to be efficacious. There have also been reports of benefit for patients with thrombotic microangiopathies associated with thrombotic thrombocytopenic purpura (49), systemic lupus erythematosus (50), and transplant-related graft-versus-host disease (51). Further study will demonstrate whether soluble TM can protect against HUS.

Disclosures

E.M.C. holds a patent for the use of the lectin-like domain of TM as an anti-inflammatory agent. The other authors have no financial conflicts of interest.

References

1. Tarr, P. I., C. A. Gordon, and W. L. Chandler. 2005. Shiga-toxin-producing *Escherichia coli* and haemolytic uraemic syndrome. *Lancet* 365: 1073–1086.
2. Noris, M., and G. Remuzzi. 2005. Hemolytic uremic syndrome. *J. Am. Soc. Nephrol.* 16: 1035–1050.
3. Karmali, M. A. 2004. Infection by Shiga toxin-producing *Escherichia coli*: an overview. *Mol. Biotechnol.* 26: 117–122.
4. Mark Taylor, C. 2008. Enterohaemorrhagic *Escherichia coli* and *Shigella dysenteriae* type 1-induced haemolytic uraemic syndrome. *Pediatr. Nephrol.* 23: 1425–1431.
5. Pennington, H. 2010. *Escherichia coli* O157. *Lancet* 376: 1428–1435.
6. Karpac, C. A., X. Li, D. R. Terrell, J. A. Kremer Hovinga, B. Lämmle, S. K. Vesely, and J. N. George. 2008. Sporadic bloody diarrhoea-associated thrombotic thrombocytopenic purpura-haemolytic uraemic syndrome: an adult and paediatric comparison. *Br. J. Haematol.* 141: 696–707.
7. Frank, C., D. Werber, J. P. Cramer, M. Askar, M. Faber, M. an der Heiden, H. Bernard, A. Fruth, R. Prager, A. Spode, et al; HUS Investigation Team. 2011. Epidemic profile of Shiga-toxin-producing *Escherichia coli* O104:H4 outbreak in Germany. *N. Engl. J. Med.* 365: 1771–1780.
8. Fukushima, H., T. Hashizume, Y. Morita, J. Tanaka, K. Azuma, Y. Mizumoto, M. Kaneno, M. Matsuura, K. Konma, and T. Kitani. 1999. Clinical experiences in Sakai City Hospital during the massive outbreak of enterohemorrhagic *Escherichia coli* O157 infections in Sakai City, 1996. *Pediatr. Int.* 41: 213–217.
9. Matsell, D. G., and C. T. White. 2009. An outbreak of diarrhea-associated childhood hemolytic uremic syndrome: the Walkerton epidemic. *Kidney Int. Suppl.* (112): S35–S37.
10. Wendel, A. M., D. H. Johnson, U. Sharapov, J. Grant, J. R. Archer, T. Monson, C. Koschmann, and J. P. Davis. 2009. Multistate outbreak of *Escherichia coli* O157:H7 infection associated with consumption of packaged spinach, August-September 2006: the Wisconsin investigation. *Clin. Infect. Dis.* 48: 1079–1086.
11. Bielaszewska, M., A. Mellmann, W. Zhang, R. Köck, A. Fruth, A. Bauwens, G. Peters, and H. Karch. 2011. Characterisation of the *Escherichia coli* strain associated with an outbreak of haemolytic uraemic syndrome in Germany, 2011: a microbiological study. *Lancet Infect. Dis.* 11: 671–676.
12. Michael, M., E. J. Elliott, J. C. Craig, G. Ridley, and E. M. Hodson. 2009. Interventions for hemolytic uremic syndrome and thrombotic thrombocytopenic purpura: a systematic review of randomized controlled trials. *Am. J. Kidney Dis.* 53: 259–272.
13. Bitzan, M. 2009. Treatment options for HUS secondary to *Escherichia coli* O157:H7. *Kidney Int. Suppl.* 75: S62–S66.
14. Lapeyraque, A. L., M. Malina, V. Fremeaux-Bacchi, T. Boppel, M. Kirschfink, M. Oualha, F. Proulx, M. J. Clermont, F. Le Deist, P. Niaudet, and F. Schaefer. 2011. Eculizumab in severe Shiga-toxin-associated HUS. *N. Engl. J. Med.* 364: 2561–2563.
15. Zoja, C., S. Buelli, and M. Morigi. 2010. Shiga toxin-associated hemolytic uremic syndrome: pathophysiology of endothelial dysfunction. *Pediatr. Nephrol.* 25: 2231–2240.
16. Esmon, C. T. 1995. Thrombomodulin as a model of molecular mechanisms that modulate protease specificity and function at the vessel surface. *FASEB J.* 9: 946–955.
17. Van de Wouwer, M., and E. M. Conway. 2004. Novel functions of thrombomodulin in inflammation. *Crit. Care Med.* 32(Suppl. 5): S254–S261.
18. Van de Wouwer, M., D. Collen, and E. M. Conway. 2004. Thrombomodulin-protein C-EPCR system: integrated to regulate coagulation and inflammation. *Arterioscler. Thromb. Vasc. Biol.* 24: 1374–1383.
19. Delvaeye, M., M. Noris, A. De Vriese, C. T. Esmon, N. L. Esmon, G. Ferrell, J. Del-Favero, S. Plaisance, B. Claes, D. Lambrechts, et al. 2009. Thrombomodulin mutations in atypical hemolytic-uremic syndrome. *N. Engl. J. Med.* 361: 345–357.
20. Conway, E. M., M. Van de Wouwer, S. Pollefeyt, K. Jurk, H. Van Aken, A. De Vriese, J. I. Weitz, H. Weiler, P. W. Hellings, P. Schaeffer, et al. 2002. The lectin-like domain of thrombomodulin confers protection from neutrophil-mediated tissue damage by suppressing adhesion molecule expression via nuclear factor kappaB and mitogen-activated protein kinase pathways. *J. Exp. Med.* 196: 565–577.
21. Van de Wouwer, M., S. Plaisance, A. De Vriese, E. Waelkens, D. Collen, J. Persson, M. R. Daha, and E. M. Conway. 2006. The lectin-like domain of thrombomodulin interferes with complement activation and protects against arthritis. *J. Thromb. Haemost.* 4: 1813–1824.
22. Fernández, G. C., M. W. Te Loo, T. J. van der Velden, L. P. van der Heuvel, M. S. Palermo, and L. L. Monnens. 2003. Decrease of thrombomodulin contributes to the procoagulant state of endothelium in hemolytic uremic syndrome. *Pediatr. Nephrol.* 18: 1066–1068.

23. Morigi, M., M. Galbusera, S. Gastoldi, M. Locatelli, S. Buelli, A. Pezzotta, C. Pagani, M. Noris, M. Gobbi, M. Stravalaci, et al. 2011. Alternative pathway activation of complement by Shiga toxin promotes exuberant C3a formation that triggers microvascular thrombosis. *J. Immunol.* 187: 172–180.
24. Zanchi, C., C. Zoja, M. Morigi, F. Valsecchi, X. Y. Liu, D. Rottoli, M. Locatelli, S. Buelli, A. Pezzotta, P. Mapelli, et al. 2008. Fractalkine and CX3CR1 mediate leukocyte capture by endothelium in response to Shiga toxin. *J. Immunol.* 181: 1460–1469.
25. Woodfin, A., M. B. Voisin, and S. Nourshargh. 2007. PECAM-1: a multi-functional molecule in inflammation and vascular biology. *Arterioscler. Thromb. Vasc. Biol.* 27: 2514–2523.
26. Privratsky, J. R., D. K. Newman, and P. J. Newman. 2010. PECAM-1: conflicts of interest in inflammation. *Life Sci.* 87: 69–82.
27. Nourshargh, S., F. Krombach, and E. Dejana. 2006. The role of JAM-A and PECAM-1 in modulating leukocyte infiltration in inflamed and ischemic tissues. *J. Leukoc. Biol.* 80: 714–718.
28. Roche, J. K., T. R. Keepers, L. K. Gross, R. M. Seaner, and T. G. Obrig. 2007. CXCL1/KC and CXCL2/MIP-2 are critical effectors and potential targets for therapy of *Escherichia coli* O157:H7-associated renal inflammation. *Am. J. Pathol.* 170: 526–537.
29. Keepers, T. R., L. K. Gross, and T. G. Obrig. 2007. Monocyte chemoattractant protein 1, macrophage inflammatory protein 1 alpha, and RANTES recruit macrophages to the kidney in a mouse model of hemolytic-uremic syndrome. *Infect. Immun.* 75: 1229–1236.
30. Turnberg, D., M. Lewis, J. Moss, Y. Xu, M. Botto, and H. T. Cook. 2006. Complement activation contributes to both glomerular and tubulointerstitial damage in adriamycin nephropathy in mice. *J. Immunol.* 177: 4094–4102.
31. Siegler, R. L. 1994. Spectrum of extrarenal involvement in postdiarrheal hemolytic-uremic syndrome. *J. Pediatr.* 125: 511–518.
32. Gallo, E. G., and C. A. Gianantonio. 1995. Extrarenal involvement in diarrhoea-associated haemolytic-uraemic syndrome. *Pediatr. Nephrol.* 9: 117–119.
33. Nathanson, S., T. Kwon, M. Elmaleh, M. Charbit, E. A. Launay, J. Harambat, M. Brun, B. Ranchin, F. Bandin, S. Cloarec, et al. 2010. Acute neurological involvement in diarrhea-associated hemolytic uremic syndrome. *Clin. J. Am. Soc. Nephrol.* 5: 1218–1228.
34. Siegler, R. L., M. Loghman-Adham, and O. D. Timmons. 1995. Acute respiratory failure in the hemolytic uremic syndrome. *Clin. Pediatr. (Phila.)* 34: 660–662.
35. Upadhyaya, K., K. Barwick, M. Fishaut, M. Kashgarian, and N. J. Siegel. 1980. The importance of nonrenal involvement in hemolytic-uremic syndrome. *Pediatrics* 65: 115–120.
36. Weiler, H., and B. H. Isermann. 2003. Thrombomodulin. *J. Thromb. Haemost.* 1: 1515–1524.
37. Abeyama, K., D. M. Stern, Y. Ito, K. Kawahara, Y. Yoshimoto, M. Tanaka, T. Uchimura, N. Ida, Y. Yamazaki, S. Yamada, et al. 2005. The N-terminal domain of thrombomodulin sequesters high-mobility group-B1 protein, a novel antiinflammatory mechanism. *J. Clin. Invest.* 115: 1267–1274.
38. Geudens, N., M. Van de Wouwer, B. M. Vanaudenaerde, R. Vos, C. Van De Wauwer, G. M. Verleden, E. Verbeken, T. Lerut, D. E. Van Raemdonck, and E. M. Conway. 2008. The lectin-like domain of thrombomodulin protects against ischaemia-reperfusion lung injury. *Eur. Respir. J.* 32: 862–870.
39. Fitzpatrick, M. M., V. Shah, R. S. Trompeter, M. J. Dillon, and T. M. Barratt. 1992. Interleukin-8 and polymorphoneutrophil leucocyte activation in hemolytic uremic syndrome of childhood. *Kidney Int.* 42: 951–956.
40. Forsyth, K. D., A. C. Simpson, M. M. Fitzpatrick, T. M. Barratt, and R. J. Levinsky. 1989. Neutrophil-mediated endothelial injury in haemolytic uraemic syndrome. *Lancet* 2: 411–414.
41. Inward, C. D., A. J. Howie, M. M. Fitzpatrick, F. Rafaat, D. V. Milford, and C. M. Taylor; British Association for Paediatric Nephrology. 1997. Renal histopathology in fatal cases of diarrhoea-associated haemolytic uraemic syndrome. *Pediatr. Nephrol.* 11: 556–559.
42. van Setten, P. A., V. W. van Hinsbergh, L. P. van den Heuvel, F. Preyers, H. B. Dijkman, K. J. Assmann, T. J. van der Velden, and L. A. Monnens. 1998. Monocyte chemoattractant protein-1 and interleukin-8 levels in urine and serum of patents with hemolytic uremic syndrome. *Pediatr. Res.* 43: 759–767.
43. Zoja, C., S. Angioletti, R. Donadelli, C. Zanchi, S. Tomasoni, E. Binda, B. Imberti, M. te Loo, L. Monnens, G. Remuzzi, and M. Morigi. 2002. Shiga toxin-2 triggers endothelial leukocyte adhesion and transmigration via NF-kappaB dependent up-regulation of IL-8 and MCP-1. *Kidney Int.* 62: 846–856.
44. Hietala, M. A., K. S. Nandakumar, L. Persson, S. Fahlén, R. Holmdahl, and M. Pekna. 2004. Complement activation by both classical and alternative pathways is critical for the effector phase of arthritis. *Eur. J. Immunol.* 34: 1208–1216.
45. Wang, Y., S. A. Rollins, J. A. Madri, and L. A. Matis. 1995. Anti-C5 monoclonal antibody therapy prevents collagen-induced arthritis and ameliorates established disease. *Proc. Natl. Acad. Sci. USA* 92: 8955–8959.
46. Okuda, T., N. Tokuda, S. Numata, M. Ito, M. Ohta, K. Kawamura, J. Wiels, T. Urano, O. Tajima, K. Furukawa, and K. Furukawa. 2006. Targeted disruption of Gb3/CD77 synthase gene resulted in the complete deletion of globo-series glycosphingolipids and loss of sensitivity to verotoxins. *J. Biol. Chem.* 281: 10230–10235.
47. Rutjes, N. W., B. A. Binnington, C. R. Smith, M. D. Maloney, and C. A. Lingwood. 2002. Differential tissue targeting and pathogenesis of verotoxins 1 and 2 in the mouse animal model. *Kidney Int.* 62: 832–845.
48. Saito, H., I. Maruyama, S. Shimazaki, Y. Yamamoto, N. Aikawa, R. Ohno, A. Hirayama, T. Matsuda, H. Asakura, M. Nakashima, and N. Aoki. 2007. Efficacy and safety of recombinant human soluble thrombomodulin (ART-123) in disseminated intravascular coagulation: results of a phase III, randomized, double-blind clinical trial. *J. Thromb. Haemost.* 5: 31–41.
49. Koga, T., D. Inoue, A. Okada, T. Aramaki, S. Yamasaki, M. Nakashima, A. Kawakami, and K. Eguchi. 2011. Successful treatment of sepsis-induced disseminated intravascular coagulation in a patient with idiopathic thrombocytopenic purpura using recombinant human soluble thrombomodulin. *Rheumatol. Int.* 31: 1657–1659.
50. Sakai, M., T. Ikezoe, K. Bandobashi, and A. Yokoyama. 2010. Successful treatment of thrombotic thrombocytopenic purpura associated with systemic lupus erythematosus with recombinant human soluble thrombomodulin. *Thromb. Res.* 126: e392–e393.
51. Inoue, Y., S. Kosugi, I. Miura, Y. Hatta, and J. Takeuchi. 2011. Successful treatment of refractory acute GVHD complicated by severe intestinal transplant-associated thrombotic microangiopathy using recombinant thrombomodulin. *Thromb. Res.* 127: 603–604.